Cell Reports, Volume *37*

Supplemental information

Expeditious recruitment of circulating memory CD8 T cells to the liver facilitates control of malaria

Mitchell N. Lefebvre, Fionna A. Surette, Scott M. Anthony, Rahul Vijay, Isaac J. Jensen, Lecia L. Pewe, Lisa S. Hancox, Natalija Van Braeckel-Budimir, Stephanie van de Wall, Stina L. Urban, Madison R. Mix, Samarchith P. Kurup, Vladimir P. Badovinac, Noah S. Butler, and John T. Harty

Figure S1. Related to Figure 1.

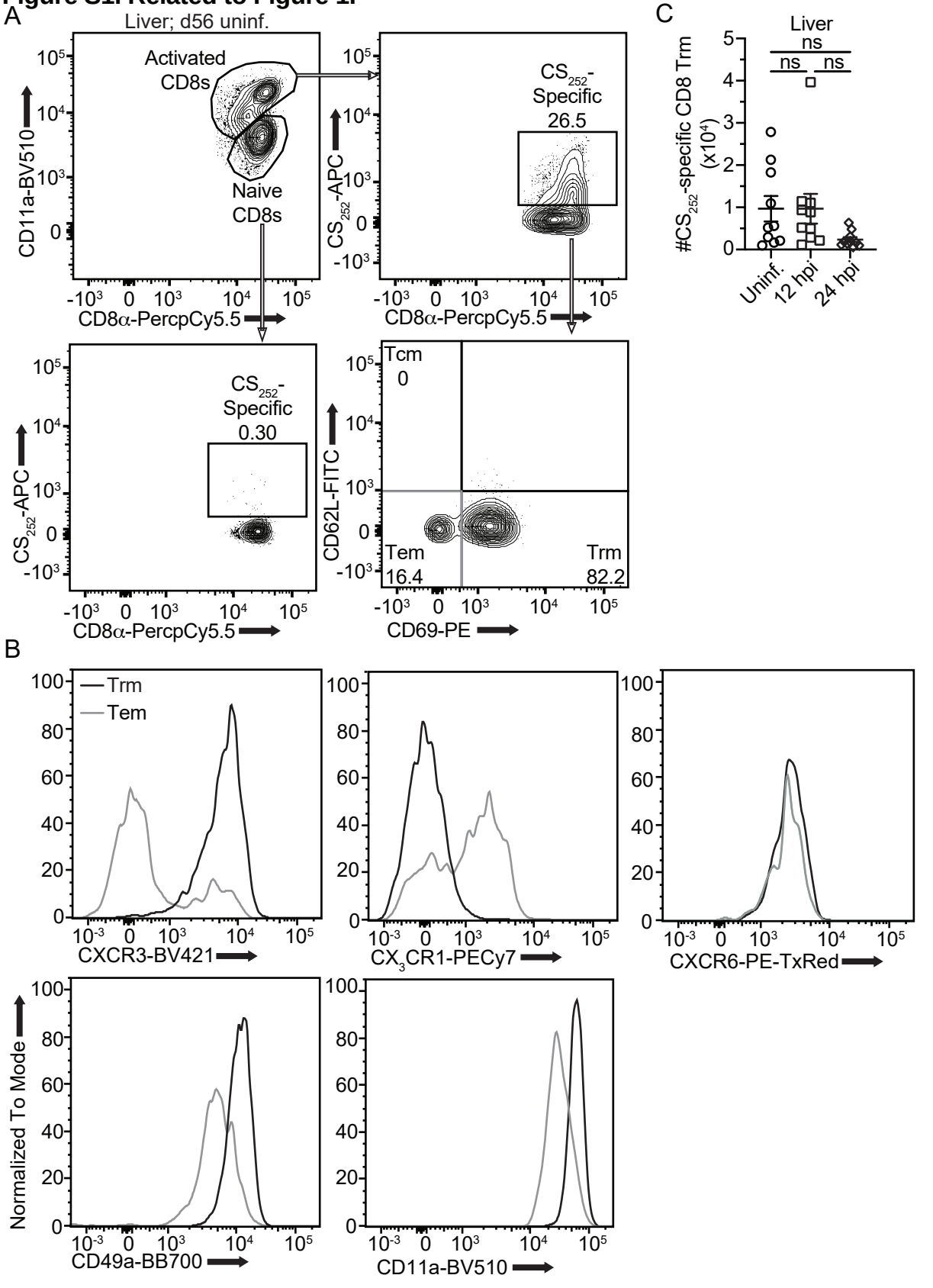

SUP FIG 1. RAS vaccination induces liver Trm and circulating Tem (Related to FIG 1).

A) Representative flow cytometry from the liver of a RAS immunized mouse 1 month post-boost. Delineation of CD8α+ cells into activated (CD11a^{hi} CD8α$^{hi/lo}$) and naïve (CD11a ^{int}CD8α^{hi}) populations (top row, left panel). CS_{252}-specific tetramer staining on activated (top row, right panel) and naïve cells (bottom row, left panel). CD62L and CD69 staining of tetramer+ cells (bottom row, right panel).

B) Representative histograms of staining of the indicated T cell phenotypic markers from the livers of RAS-vaccinated mice 56 days after the first RAS vaccination.

C) Numbers of CS_{252}-specific Trm cells recovered from livers of RAS-vaccinated mice at 0, 12, & 24 hpi with *Pb* sporozoites.

All data are combined from two independent experiments, each with at least three mice per group. Each dot represents an individual mouse and mean ± SEM are depicted. (C) One way ANOVA comparing the mean of each column to the mean of every other column was performed. ns $p > 0.05$.

Figure S2. Related to Figure 2.

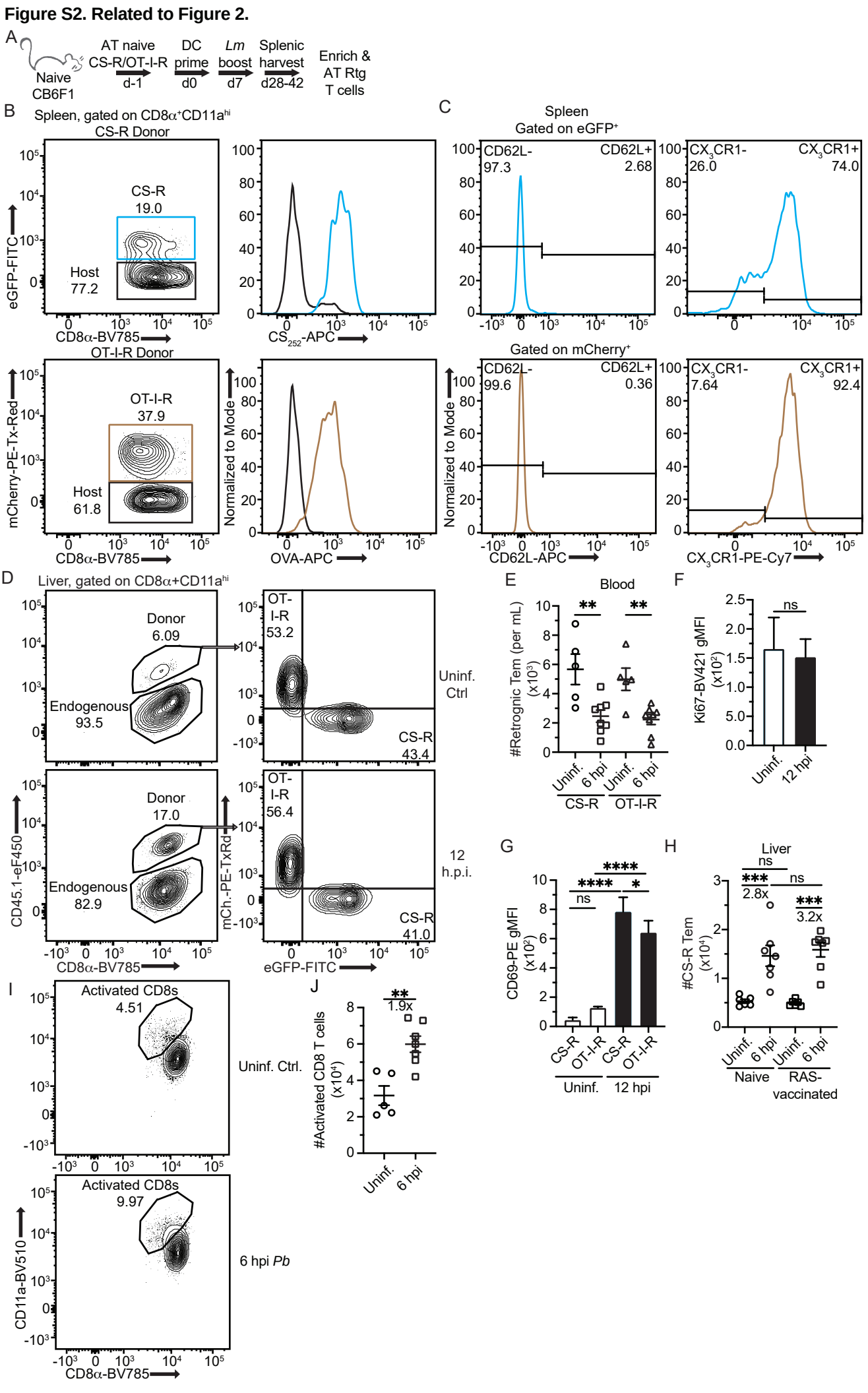

SUP FIG 2 Circulating retrogenic memory CD8 T cells can be tracked during liver infection (Related to Fig 2).

A) Experimental schematic of CD45.1/2 Rtg memory CD8 T cell generation in CD45.2/2 CB6F1 mice. Naïve Rtg T cells were transferred to recipient mice followed by immunization with peptide pulsed dendritic cells (DCs) and attenuated recombinant *Lm* expressing secreted CS_{252} or OVA peptide. Donor splenocytes from immunized mice were enriched for $CD8\alpha^+$ T cells prior to adoptive transfer (AT) and analyses in the liver.

B) Representative flow cytometry demonstrating fluorescence of splenic Rtg T cells and their ability to bind to respective tetramers 28 days post-*Lm*-CS_{252}/*Lm*-OVA vaccination.

C) Representative flow cytometry demonstrating patterns of CD62L and CX_3CR1 expression by splenic CS-R cells 28 days post-*Lm*-CS_{252} vaccination.

D) Representative flow cytometry showing gating strategy to identify Rtg donor cells in recipient mice. Rtg cells were co-AT in equal amounts as shown in Figure 3A. Events were derived from live $CD8\alpha^+$ singlets.

E) Quantification of Rtg Tem cells recovered from the blood of mice 6 hpi with *Pb* sporozoites. Numbers are presented as per mL of blood volume.

F) Quantification of Ki67 expression by liver-localized CS-R Tem cells 12 hp. with *Pb* sporozoites. One representative result is shown from two experiments; 4 mice per group.

G) Quantification of CD69 expression by liver localized Rtg T cells in uninfected mice or mice 12 hpi with *Pb* sporozoites. One representative result is shown from two experiments; 3-4 mice per group.

H) Quantification of liver-localized CS-R Tem cells recovered from previously naïve or RAS-vaccinated mice 6 hpi with *Pb* sporozoites.

I) Representative flow cytometry demonstrating endogenous liver-localized activated CD8 T cells in previously naïve mice that subsequently received adoptive transfer of CS-R Tem cells. The parent population is live singlet $CD8\alpha^+CD45.1^-$ events.

J) Quantification of liver-localized endogenous activated CD8 T cells recovered from mice 6 hpi with *Pb* sporozoites.

All data except F) and G) are combined from two independent experiments, each with 2-5 mice per group. Each dot represents an individual mouse and mean ± SEM are depicted. F) and G) display a representative experiment selected from two independent experiments and mean ±SD are depicted. G), H) One way ANOVA (Turkey's post-hoc) comparing the mean of each column to the mean of every other column was performed. E), F), J) Unpaired two-tailed t-tests assuming similar SD were performed. *$p \leq 0.05$, **$p \leq 0.01$, ***$p \leq 0.001$, ****$p \leq 0.0001$, n.s. $p > 0.05$.

Figure S3. Related to Figure 4.

A

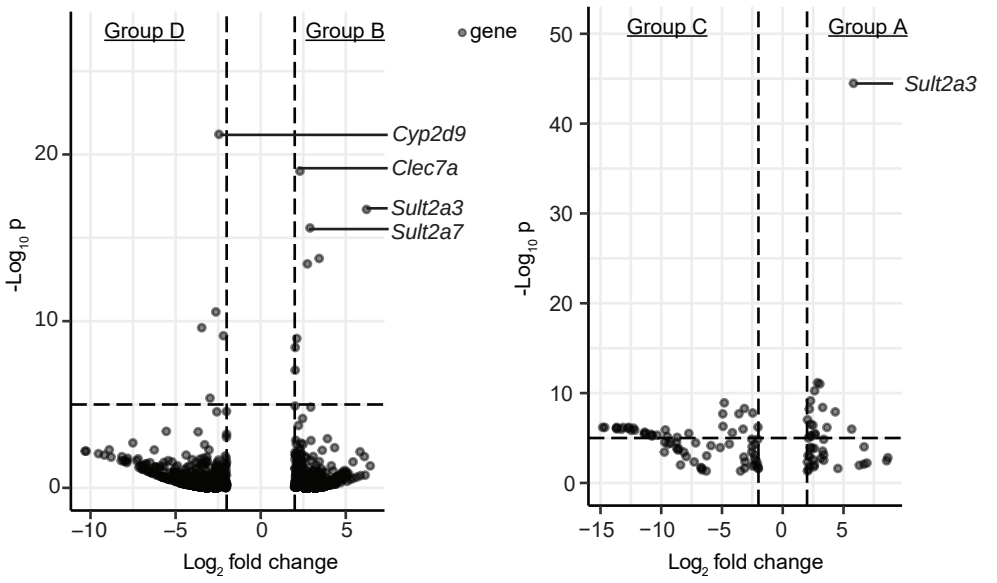

SUP FIG 3. RAS vaccination status has minimal impact on the liver transcriptional profile (Related to FIG 4).

A) Volcano plots comparing individual gene expression differences between various groups. Genes with a log2 fold change between -2 and 2 are excluded. Genes of particular interest are labeled. Dashed lines indicate thresholds of significance for log2 fold change (x axis, ± 2) and adjusted p value (y axis, <0.05).

Sup Fig 4. Related to Figure 5.

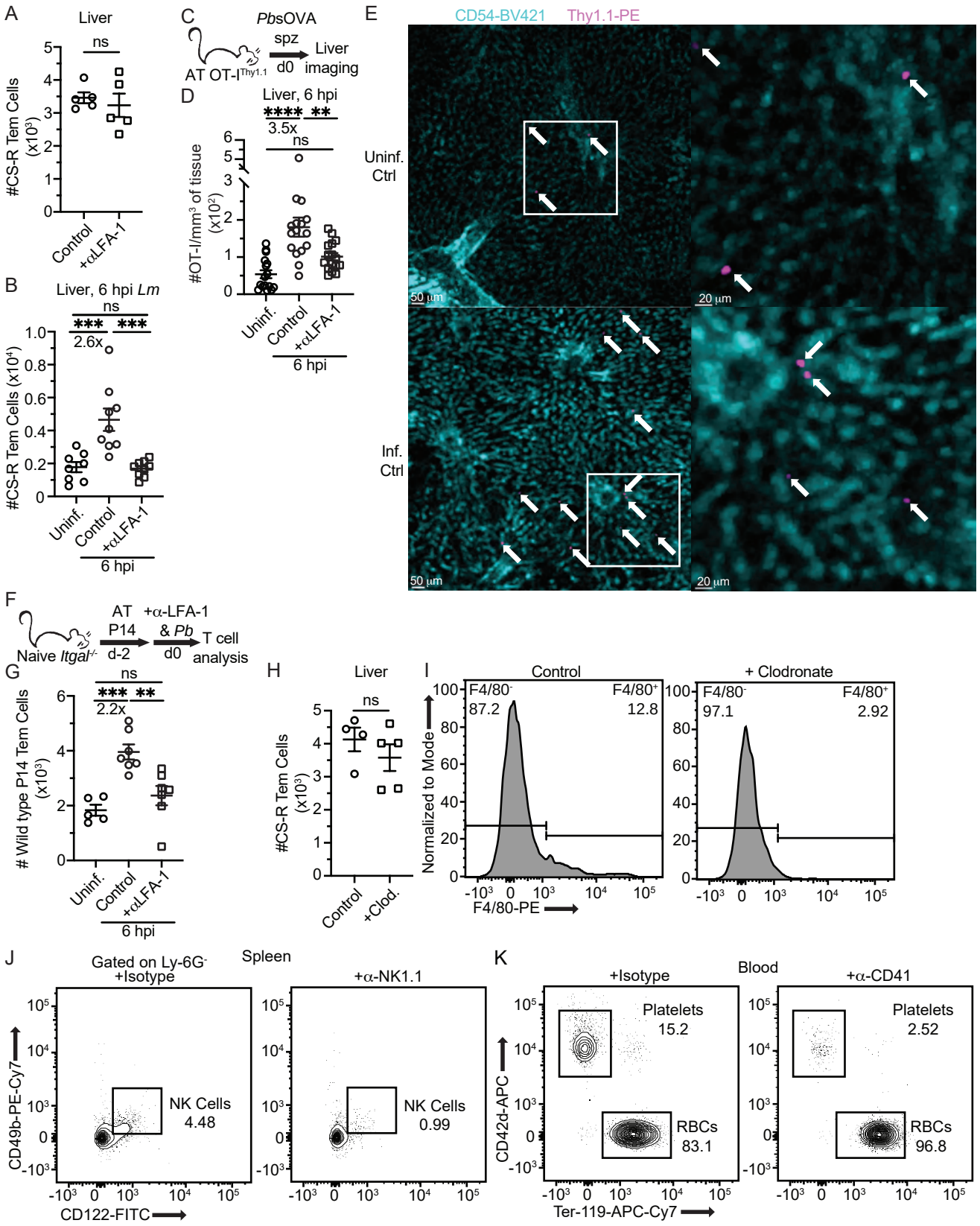

SUP FIG 4. CD8 T cell-intrinsic LFA-1 mediates rapid Tem recruitment (Related to FIG 5).

A) Mice received adoptive transfer of $5x10^5$ CS-R Tem cells, and were treated with isotype control or blocking α-LFA-1 antibody 2 days later. CS-R Tem cells were enumerated from the livers 3 hours after treatment.

B) Mice generated as in 4A received challenge with 10^6 cfu of virulent *Lm*-OVA with or without LFA-1 blockade. Quantification of liver-localized CS-R Tem cells 6hpi is shown.

C) Experimental schematic for microscopy experiments. 10^5 Thy1.1$^+$ OT-I cells harvested from the spleens of DC-*Lm*-OVA-vaccinated donor mice were adoptively transferred into naïve Thy1.2$^+$ C57Bl/6 mice before challenge with $3x10^4$ transgenic *Pb*sOVA sporozoites, which express secreted OVA during liver-stage infection that can be presented by hepatocyte MHC-I.

D) Quantification of Thy1.1 OT-I cells in the liver slices of different groups of mice. Each dot represents a number from a single image, with two images captured per slice and two slices imaged per mouse (a total of 4 mice in each group).

E) Representative $1mm^2$ images captured from uninfected and infected control mouse liver slices. Scale bar is 50μm. Blue labels CD54 (expressed constitutively by liver sinusoidal endothelium) and pink labels Thy1.1$^+$ OT-I memory CD8 T cells (indicated by white arrows). Selected zoomed in images captured from the areas highlighted by white boxes are displayed to the right.

F), G) Quantification of liver-localized WT P14 Tem cells recovered from LFA-1 KO host mice 6 hpi with $3x10^4$ *Pb* sporozoites with or without LFA-1 blockade. P14 cells were harvested from the spleens of mice that previously received P14 AT and subsequent DC-*Lm*-gp33-vaccination.

H) Mice received adoptive transfer of $5x10^5$ CS-R Tem cells and some were treated with clodronate liposomes 2 days later. CS-R Tem cells were enumerated from the livers 1 day after treatment.

I) Representative flow cytometry from the livers of control or clodronate liposome-treated mice 1 day post treatment. F4/80$^+$ events on CD3$^-$B220$^-$Ly-6C$^-$Ly-6G$^-$ gated cells are displayed.

J) Representative flow cytometry from the spleens of isotype control or α-NK1.1-treated mice 1 day post-depletion. CD122 and CD49b expression on Ly-6G- spleen cells are displayed.

K) Representative flow cytometry from the blood of isotype control or α-CD41-treated 2 hours post-depletion. Platelets are Ter-119$^-$CD42d$^+$.

All data depict two independent experiments collated, with 2-5 mice per group and are presented as mean ± SEM. K), L), and M) show representative findings from their respective experiments. B), D), G) One way ANOVA (Turkey's post-hoc) comparing the mean of each column to the mean of every other column was performed. A), I), J), Unpaired two-tailed t-tests assuming similar SD were performed. *p≤ 0.05, **p ≤ 0.01, ***p ≤ 0.001, ****p ≤ 0.0001, ns p > 0.05.

Figure S5. Related to Figure 5.

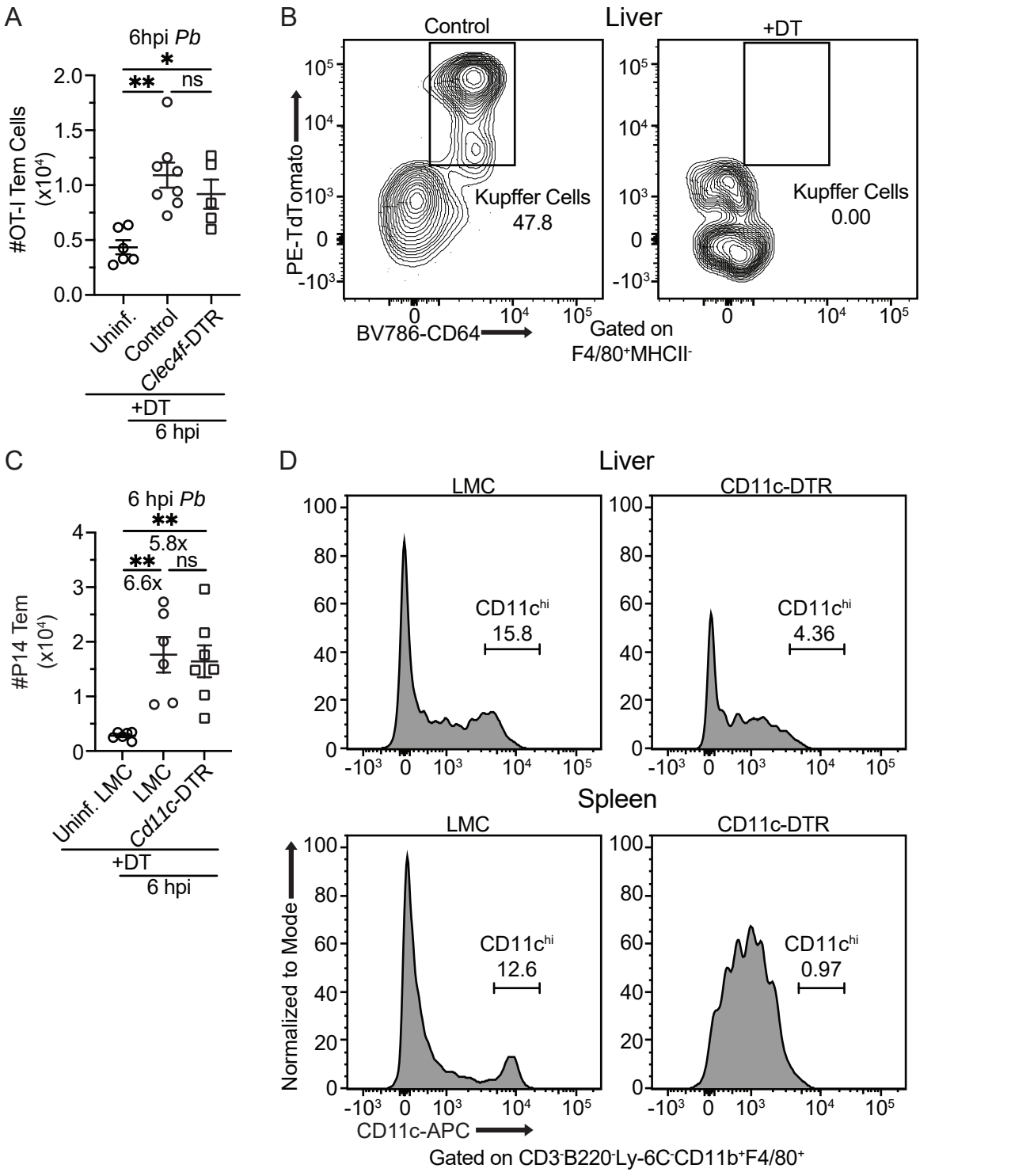

SUP FIG 5. Kupffer cells and CD11c^{hi} cells do not impact Tem recruitment during liver-stage malaria (Related to FIG 5).

(A) eGFP OT-I cells were enriched from the spleens of DC-*Lm*-OVA-vaccinated wild type C57Bl/6 mice and adoptively transferred into wild type or Clec4f-DTR recipients. Mice were treated with 200 ng of diphtheria toxin (DT) 1 day post-transfer. Some were challenged with 3x10^4 *Pb* sporozoites 1 day post DT treatment. eGFP OT-I cells were enumerated from livers 6 hpi via flow cytometry.

(B) Representative flow cytometry from the livers of control or DT-treated *Clec4f*-DTR mice 1 day post-depletion. Kupffer cells are F4/80$^+$MHC-II$^-$CD64$^+$, and express TdTomato$^+$ in *Clec4f*-DTR mice.

(C) Quantification of liver-localized wild type P14 Tem cells recovered from littermate control (LMC) and CD11c-DTR mice 6 hpi with 3x10^4 *Pb* sporozoites. Mice were treated with 200ng DT 1 day prior to infection. P14 CD8 T cells were generated as in (S4C).

(D) Representative flow cytometry from the livers (top) and spleens (bottom) of LMC or CD11c-DTR mice 1 day post-DT treatment.

All data depict two independent experiments collated, with 2-4 mice per group and are presented as mean ± SEM. (A), (C) One way ANOVA (Turkey's post hoc) comparing the mean of each column to the mean of every other column was performed. *p≤ 0.05, **p ≤ 0.01, ***p ≤ 0.001, ****p ≤ 0.0001, ns p > 0.05.